

Analytical and numerical analysis of the behaviour of RC beams flexural strengthened with CFRP

J.A.O. Barros, S.J.E. Dias & J.L.T. Lima
 ISISE, University of Minho, Guimarães, Portugal

ABSTRACT: Experimental research regarding the flexural strengthening of reinforced concrete (RC) structures with Carbon Fibre Reinforced (CFRP) systems using the Externally Bonded Reinforcing (EBR) and the Near Surface Mounted (NSM) techniques has been carried out at the University of Minho. Considering the experimental results of this research, the performance of the ACI and *fib* formulations for the EBR flexural strengthening was appraised in this paper. The same was done in terms of NSM technique adopting for the CFRP debonding strain a value that is 70% of the CFRP ultimate strain, according to the recommendations of the ACI Committee 440. However, the experimental results show that the CFRP debonding strain is dependent on the CFRP percentage and existing longitudinal steel reinforcement ratio. To estimate an equation for the prediction of the CFRP debonding strain, which takes into account these parameters, a numerical model was applied to the simulation of the tests carried out.

1 SERIES OF RC BEAMS

Figure 1 represents the geometry of the beam type, the distinct reinforcement arrangements and the number and position of the CFRP strengthening systems of the different cross sections of the beams of an experimental program carried out at the University of Minho. The obtained results were also used to appraise the capability of the ACI (2007) and *fib* (2001) analytical models for the prediction of the contribution of the EBR and NSM techniques for the flexural strengthening of RC beams.

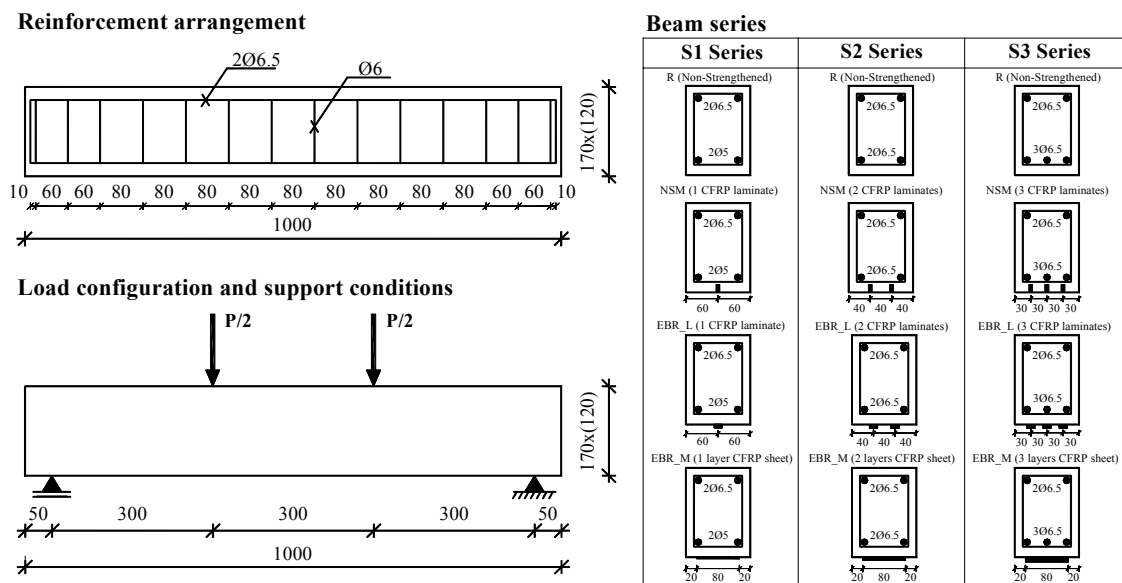


Figure 1. Beams used for analytical and numerical analysis.

The concrete average compressive strength, f_{cm} , evaluated in cylinders of 300 mm height and 150 mm diameter, was 52.2 MPa. From the tensile tests with specimens of $\phi 5$ and $\phi 6.5$ steel bars, a yield stress, f_{sym} , of 788 MPa ($\phi 5$) and 627 MPa ($\phi 6.5$), and a ultimate strength, f_{sum} , of 890 MPa ($\phi 5$) and 765 MPa ($\phi 6.5$) were obtained. Two CFRP systems were used in the present work: unidirectional wet lay-up sheets (0.111×80 mm² cross sectional area per layer) for the beams with EBR_M and precured laminates (1.4×9.6 mm² cross sectional area per strip) for the beams EBR_L and NSM_L (see Figure 1). According to the manufacturer, the values of the tensile strength (f_{fu}^*), elastic modulus (E_f) and ultimate tensile strain (ε_{fu}^*) for the wet lay-up sheets are equal to 3700 MPa, 240 GPa and 15‰, respectively. From the tests carried out with CFRP laminates, the following average values were obtained: $f_{fu}^* = 2740$ MPa, $E_f = 158.8$ GPa and $\varepsilon_{fu}^* = 17$ ‰.

2 APPRAISAL OF THE ACI AND *FIB* ANALYTICAL FORMULATIONS

Taking the results obtained in the tested beams strengthened with the EBR technique, the performance of the analytical formulations proposed by ACI (2007) and *fib* (2001) was appraised. The load carrying capacity of EBR strengthened RC beams can be estimated from the design resisting bending moment of the cross section of these beams (M_{Rd}). ACI and *fib* analytical formulations propose the following respective equations:

$$M_{Rd} = \phi \left(A_{sl} f_{syd} (d_s - \beta_1 x / 2) + \gamma_f A_f f_{fe} (h - \beta_1 x / 2) \right) \quad \text{ACI} \quad (1)$$

$$M_{Rd} = A_{sl} f_{syd} (d_s - \delta_G x) + A_f f_{fe} (h - \delta_G x) \quad \text{fib} \quad (2)$$

where A_f is the CFRP cross sectional area, A_{sl} and f_{syd} are the cross sectional area and the design yielding stress of the longitudinal tensile steel bars, h is the height of the beam cross section, x is the position of the neutral axis, f_{fe} is the effective tensile stress at ultimate conditions in the FRP ($f_{fe} = E_f \varepsilon_{fe}$), ϕ is a strength reduction factor to attend the ductility level of the cross section, and $\gamma_f = 0.85$ is an additional safety factor for the flexural-strengthening contribution of the FRP reinforcement. The parameters d_s and d_f are the effective depth of the longitudinal steel bars and FRP systems, respectively. The term β_1 is the ratio of the depth of the equivalent rectangular stress block to the depth of the neutral axis (ACI 2007) and δ_G is the stress block centroid coefficient (*fib* 2001). In equations (1) and (2) it was assumed that the thickness of the FRP laminates and sheets, as well as the corresponding adhesive materials can be neglected for the evaluation of the internal arm of the FRP system.

The FRP effective strain, ε_{fe} , is evaluated from:

$$\varepsilon_{fe} = \varepsilon_{cu} \left(\frac{d_f - x}{x} \right) - \varepsilon_{ci} \leq \varepsilon_{fd} \quad (3)$$

where ε_{cu} is the maximum acceptable concrete compressive strain (=0.003 in the ACI formulation and =0.0035 in the *fib* formulation), ε_{ci} is the initial strain of the concrete substrate, ε_{fd} is the debonding strain of externally bonded FRP reinforcement.

In the ACI formulation the parameter ε_{fd} can be obtained from the following equation (ACI 2007):

$$\varepsilon_{fd} = 0.42 \sqrt{\frac{f_c'}{n E_f t_f}} \leq 0.9 \varepsilon_{fu} \quad (4)$$

where f'_c is the specified compressive strength of the concrete, n is the number of plies of FRP flexural reinforcement at the cross section of the member where the resisting bending moment is being computed, t_f is the thickness of the FRP material and $\varepsilon_{fu} = C_E \varepsilon_{fu}^*$ is the FRP design rupture strain, in which C_E is an environmental-reduction factor.

In the *fib* approach the debonding strain is calculated according to the following equation:

$$\varepsilon_{fd} = \alpha c_1 k_c k_b \sqrt{\frac{f_{ctm}}{n E_f t_f}} \leq \varepsilon_{fu} \quad (5)$$

where f_{ctm} is the mean value of the concrete tensile strength (for the concrete of the tested beams the value adopted was $f_{ctm} = 3.75$ MPa), $\varepsilon_{fu} = \varepsilon_{fu}^* / \gamma_f$ is the FRP design rupture strain, in which γ_f is CFRP material safety factor, α is a reduction factor, equal to 0.9, to account for the influence of inclined cracks on the bond strength ($\alpha = 1$ in beams with sufficient internal and external shear reinforcement and in slabs), c_1 is an empirical factor assumed to be 0.64 for FRP, k_c is a factor accounting for the state of concrete compaction ($k_c = 1.0$, but for FRP bonded to concrete faces with low compaction, e.g. faces not in contact with the formwork during casting, $k_c = 0.67$) and k_b is a geometry factor:

$$k_b = 1.06 \sqrt{\left(2 - \frac{b_f}{b}\right) / \left(1 + \frac{b_f}{400}\right)} \geq 1.0 \quad (6)$$

where b_f is the width of the FRP system and b the width of the beam cross section.

When the design values of these parameters are used (see Table 1), the values of the beam maximum load carrying capacity of the tested beams ($P_{max}^{ana} = M_{Rd} / 0.15$, see Figure 1), obtained from ACI and *fib* formulations, are compared to the experimental ones in Figure 2. This figure shows that both ACI and *fib* formulations provide some unsafe results for some EBR_M strengthening arrangements. For the EBR technique using laminates (EBR_L), both formulations provide safe results.

Table 1. Properties of the materials.

| Materials | Average values (experimental values) | | Design values | |
|---------------|--|---------------------|---|------------------------------------|
| | | | ACI formulation | <i>fib</i> formulation |
| Concrete | $f_{cm} = 52.2$ MPa | | $f'_c = 42.9$ MPa ^a | $f_{cd} = 29.5$ MPa ^b |
| Steel | $\phi 5$ | $f_{sym} = 788$ MPa | $f_{syd} = f_y = 685.2$ MPa ^c | $f_{syd} = 685.2$ MPa ^c |
| | $\phi 6.5$ | $f_{sym} = 627$ MPa | $f_{syd} = f_y = 545.2$ MPa ^c | $f_{syd} = 545.2$ MPa ^c |
| CFRP laminate | $E_f = 158.8$ GPa; $\varepsilon_f = 17\%$ ^o | | $E_f = 158.8$ GPa; $\varepsilon_f = 17\%$ ^d | |
| CFRP sheet | - | | $E_f = 240$ GPa; $\varepsilon_f = 15\%$ ^{d, e} | |

^a $f'_c = (f_{cm} - 5) / 1.1$ (ACI 318 2002); ^b $f_{cd} = (f_{cm} - 8) / 1.5$ (CEB-FIP 1993); ^c $f_{syd} = f_{sym} / 1.15$; ^d In ACI formulation the strain value was multiplied by the environmental-reduction factor $C_E = 0.95$ (ACI 2007) and in *fib* formulation the strain value was divided by the CFRP material safety factor $\gamma_f = 1.2$ (*fib* 2001); ^e According to the supplier.

For the NSM technique, the ACI (2007) document recommends the use of $\varepsilon_{fd} = 0.7 \varepsilon_{fu}$. If this value is used, the ACI and *fib* analytical formulations (Equations (1) and (2)) lead the results indicated in Figure 2 (if design values are used for the materials properties). From the analysis of these values it can be concluded that both ACI and *fib* formulations provide safe results (the exception is the values for the beam of the third series). Furthermore, ACI formulation provides

larger $P_{max}^{exp}/P_{max}^{ana}$ values than *fib* approach. A relevant aspect is the decrease of the $P_{max}^{exp}/P_{max}^{ana}$ with the increase of the $\rho_{l,eq}$, illustrated in Figure 3, where $\rho_{l,eq} = A_{sl}/(bd_s) + (A_f E_f / E_s) / (bd_f)$ is the reinforcement ratio provided by both the tensile steel bars and NSM laminates. This indicates that the debonding strain decreases with the increase of $\rho_{l,eq}$.

To obtain a relationship between $\varepsilon_{fd} / \varepsilon_{fu}$ and $\rho_{l,eq}$, a numerical model was used, able of fitting, with high accuracy, the force-displacement relationship obtained in the experimental tests. From these numerical simulations the maximum strain at failure of the beams was determined, which are used as ε_{fd} values. The applied numerical model is briefly described in the next section, but a detailed exposition can be found elsewhere (Barros & Fortes 2005).

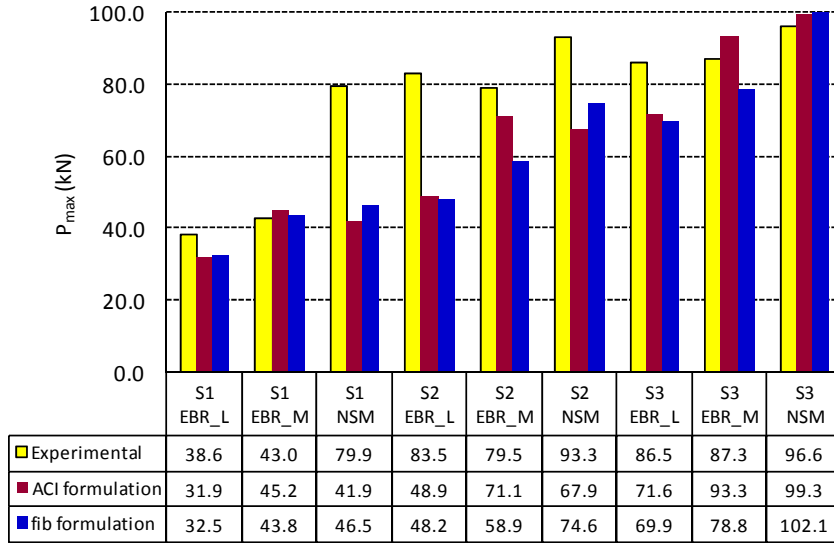


Figure 2. Experimental versus analytical maximum forces, in kN, (design values for the material properties).

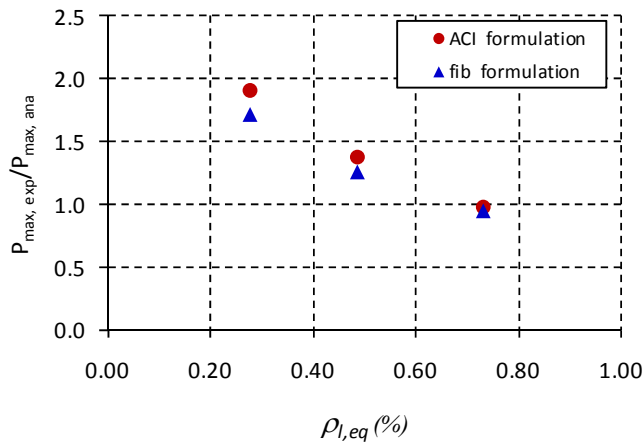


Figure 3. Relationship between $P_{max}^{exp}/P_{max}^{ana}$ and $\rho_{l,eq}$ for the beams with NSM laminates.

3 NUMERICAL SIMULATION

Previous works (Barros & Fortes 2005, Barros *et al.* 2006) shown that, using a cross section layered model that takes into account the constitutive laws of the intervening materials, and the cinematic and the equilibrium conditions, the deformational behaviour of structural elements failing in bending can be predicted from the moment-curvature relation, $M - \chi$, of the represen-

tative cross sections of these elements, using the algorithm described elsewhere (Barros & Fortes 2005). To evaluate the $M - \chi$ relationship, the beam cross section was discretized in layers of 1 mm thickness. The tested beams were discretized in sixty Euler-Bernoulli beam elements of two nodes per element. The tangential stiffness matrix of the beam was obtained by assembling the tangential stiffness matrix of these elements. The updated flexural stiffness taking part in the tangential stiffness matrix of each element was obtained from the $M - \chi$ relationship corresponding to the cross section of this element.

To simulate the concrete compression behaviour, the stress-strain relationship recommended by CEB-FIP model code was used (CEB-FIP 1993). Up to the concrete tensile strength, f_{ct} , the concrete was assumed as behaving linearly. The behaviour of the concrete layers in softening and in stiffening was simulated by the trilinear diagram represented in Figure 4. The data adopted for defining the softening and the stiffening trilinear diagram of the post-cracking behaviour of the concrete layers, used in the numerical simulation, is indicated in Table 2. Using the values of the properties of the steel bars and CFRP systems indicated in Section 1, a linear-parabola and a linear stress-strain diagram were defined to model the behaviour of these respective materials.

Due to space limitation only the experimental and numerical load-mid span deflection curves of the NSM beam of S2 series are compared in Figure 5, but the high level of accuracy obtained in this simulation was also achieved in the remaining beams.

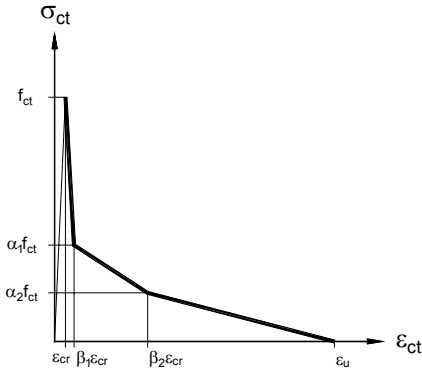


Figure 4. Trilinear stress-strain diagram to model the concrete post-cracking behaviour.

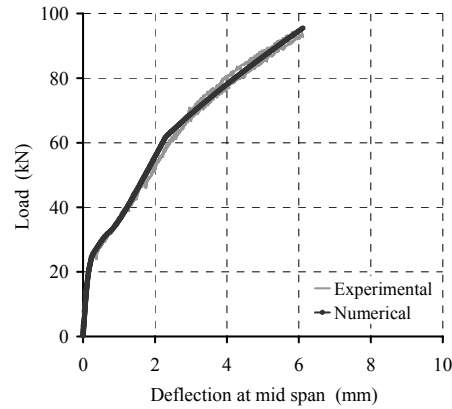


Figure 5. Experimental versus numerical force-deflection curves of the NSM beam of the S2 series.

Table 2. Values used to define the softening and the stiffening trilinear stress-strain diagram.

| Beam | Compression | | Tension | Softening | | | | | Stiffening | | | | |
|----------|-------------------|----------------|-------------------|------------|------------|-----------|-----------|---------------------|------------|------------|-----------|-----------|---------------------|
| | f_{cm} (MPa) | E_c (GPa) | f_{ct} (MPa) | α_1 | α_2 | β_1 | β_2 | ϵ_u (‰) | α_1 | α_2 | β_1 | β_2 | ϵ_u (‰) |
| S2 - NSM | 52.2 | 36.1 | 3.16 | 0.4 | 2.0 | 0.2 | 10.0 | 5.19 | 0.7 | 10.0 | 0.4 | 15 | 14.3 |

From the numerical simulation the following equation was obtained:

$$\frac{\epsilon_{fd}}{\epsilon_{fu}} = 1.987e^{-2.469\rho_{l,eq}} \quad (7)$$

which shows a tendency for an exponential decrease of the $\epsilon_{fd}/\epsilon_{fu}$ ratio with the increase of $\rho_{l,eq}$.

Using the ϵ_{fd} values obtained from Eq. (7), the P_{max}^{ana} was obtained for the NSM beams, using the ACI and *fib* formulations. In Table 3, these values are compared to the P_{max}^{exp} values recorded

in the experimental tests, from which it can be verified that, if ε_{fd} is estimated using Eq. (7), the $P_{max}^{exp}/P_{max}^{ana}$ values were greater than the unitary value and much more uniform than those determined from the use of ACI Committee 440 recommendation. In square brackets are indicated the values assuming $\varepsilon_{fd} = 0.7 \varepsilon_{fu}$, as recommended by ACI 440 (2007).

Table 3. Experimental versus analytical values of the maximum load (design values).

| Beam's series | | Experimental P_{max}^{exp} (kN) | ACI formulation | | | <i>fib</i> formulation | | |
|---------------|-----|---|-------------------------------|-----------------------------|-------------------------------|------------------------------|-----------------------------|-------------------------------|
| | | | ε_{fd} (‰) | P_{max}^{ana} (kN) | $P_{max}^{exp}/P_{max}^{ana}$ | ε_{fd} (‰) | P_{max}^{ana} (kN) | $P_{max}^{exp}/P_{max}^{ana}$ |
| S1 | NSM | 79.9 | 17.00 ^a [11.31] | 47.5 ^a [41.9] | 1.68 [1.91] | 17.00 ^b [9.92] | 55.6 ^b [46.5] | 1.44 [1.72] |
| S2 | NSM | 93.3 | 10.19 [11.31] | 64.1 [67.9] | 1.46 [1.37] | 10.19 [9.92] | 75.7 [74.6] | 1.23 [1.25] |
| S3 | NSM | 96.6 | 5.55 [11.31] | 68.9 [99.3] | 1.40 [0.97] | 5.55 [8.95] | 81.9 [102.1] | 1.18 [0.95] |

^a ACI formulation: $\varepsilon_{fd} \leq 0.9\varepsilon_{fu} = 0.9 \times 0.95 \times 17 = 14.54\%$. ^b *fib* formulation: $\varepsilon_{fd} \leq \varepsilon_{fu}/1.2 = 17/1.2 = 14.17\%$.

4 CONCLUSIONS

In this paper the performance of the ACI and *fib* formulations for the EBR flexural strengthening was appraised. Some unsafe contributions of the CFRP systems were predicted for the EBR technique using wet-lay up sheets. ACI and *fib* formulations provide safe results for the EBR when using laminates for the flexural strengthening.

With the purpose of allowing that ACI and *fib* formulations can predict the contribution of the NSM laminates for the flexural strengthening of RC beams, a relationship was established between the CFRP debonding strain, ε_{fd} (maximum strain able to apply to the laminates in terms of debonding), and a reinforcement parameter ($\rho_{l,eq}$) that takes into account the percentage of CFRP laminates and the percentage of existing longitudinal tensile steel bars, using a numerical model. Using this relationship for the determination of the ε_{fd} , the ACI and *fib* formulations provided more homogeneous values for the $P_{max}^{exp}/P_{max}^{ana}$ ratio than when assuming $\varepsilon_{fd} = 0.7 \varepsilon_{fu}$, and greater than the unitary value, where P_{max}^{exp} and P_{max}^{ana} are the maximum forces registered in the experimental tests and those obtained from the analytical models.

5 REFERENCES

- ACI Committee 318, "Building code requirements for structural concrete and commentary", American Concrete Institute, Reported by ACI Committee 118, 2002.
- ACI Committee 440. 2007. Guide for the design and construction of externally bonded FRP systems for strengthening concrete structures. American Concrete Institute.
- Barros, J.A.O., Oliveira, J.T., Lourenço, P.J.B. and Bonaldo, E. 2006. Flexural behavior of reinforced masonry panels. *ACI Structural Journal*, 13(3), 418-426.
- Barros, J.A.O. and Fortes, A.S. 2005. Flexural strengthening of concrete beams with CFRP laminates bonded into slits. *Journal Cement and Concrete Composite*, 27(4), 471-480.
- CEB-FIP Model Code. 1993. Comité Euro-International du Béton, Bulletin d'Information n° 213/214.
- fib* - Bulletin 14. 2001. Externally bonded FRP reinforcement for RC structures. Technical report by Task Group 9.3 FRP (Fiber Reinforced Polymer) reinforcement for concrete structures, Fédération Internationale du Béton - *fib*, 130 pp.